Design and Synthesis of 4-Substituted Indolo[3,2-*e*][1,2,3]triazolo[1,5-*a*]pyrimidine Derivatives with Antitumor Activity

Antonino Lauria, Chiara Patella, Gaetano Dattolo, and Anna Maria Almerico*

Dipartimento Farmacochimico, Tossicologico e Biologico - Università di Palermo, Via Archirafi 32, 90123 Palermo, Italy

Received August 2, 2007

New derivatives of the indolo[3,2-*e*][1,2,3]triazolo[1,5-*a*]pyrimidine system, substituted in the 4 position, were designed as novel antitumor agents because of their theoretical capability to form stable complexes with DNA fragments. The calculated free energies of binding were found in the range –12.76 → −39.68 Kcal/mol. The docking studies revealed a common binding mode with the chromophore intercalated between GC base pairs, whereas the side chain lies along the minor groove. Compounds, selected on the basis of the docking studies and suitably synthesized, showed antiproliferative activity against each type of tumor cell line investigated, generally in the low micromolar range. The more active derivatives were shown to be **1eJ** and **1eL**, endowed with significant antiproliferative activity against the renal and CNS subpanels, respectively. A mechanism of action closely related to the DNA-interacting drugs can be supposed, although, alternative mechanisms, similar to those of the anthracyclines, can also operate.

Introduction

DNA represents one of the more important molecular cellular targets of several chemotherapeutic drugs. Molecular recognition of DNA by small molecules and proteins is a fundamental problem in drug design. Polycyclic heterocycles having a planar structure can be effective pharmacophore moieties of DNA-interactive drugs because they can insert between the stacked base paired oligonucleotides. Moreover, if they bear suitable side chains, further interactions of these ligands with the other important architectural feature of DNA, its minor groove, can be envisaged.

Among the different classes of antitumor drugs that interact with DNA, the actinomycins, a family of chromopeptide antibiotics, represent a peculiar one that combines the two above-mentioned features. The most representative derivative, Dactinomycin (Actinomycin D), has been extensively investigated and its sequence specificity has been analyzed in detail by a variety of methods, including chemical footprinting,[1] NMR,[2] X-ray crystallography,[3] and photoaffinity cross-linking.[4,5] It binds to double-stranded DNA and the phenoxazone moiety intercalates between bases, whereas the peptide substituents lie in the minor groove.[6] The biological activity appears to depend on the very slow rate of dissociation of the complex between DNA and the drug, which reflects the intermolecular hydrogen bonds, the planar interaction between the purine rings and the chromophore, and the numerous van der Waals interactions between the polypeptide side chain and the DNA.

In this context, we have already been interested in the design and development of several types of tricyclic/tetracyclic derivatives presenting a triazolo-pyrimidine moiety further condensed with a pyrrole/indole ring,[7–10] stucturally correlated to classes of DNA-intercalating agents. The synthetic approach to these new heterocyclic ring systems was exhaustively investigated by us during these studies: it always involved a domino reaction between an azido-pyrrole/indole-*ortho*-carboxylate and substituted acetonitriles. The azido moiety acts as a 1,3-dipolar reagent in cycloaddition reactions with dipolarophiles such as anions obtained from methylene active derivatives. The intermediate resulting from the cycloaddition reaction is a 1-(2-carboxyethyl-heteroaryl)-2-aminotriazole, which presents an amino group able to give rise to the pyrimidine ring, being within reacting distance to the carboxylate function. We have already shown that this type of reaction can be used in the pyrrole/indole series and have demonstrated that the nature of the substrate and the reaction conditions can widely influence the nature of the reaction products. Although, in the presence of the same type of complexity (two rings formed in sequence), for this type of domino reaction, the bond-forming economy greatly depends on the nature of the starting material (pyrrole/indole) and on the substitution pattern. However, a minor modification of the experimental procedure allows the reaction to become suitable for a general application in both series. By this approach we were able to synthesize derivatives of several new systems such as (pyrrolo[3,4-*e*] and pyrrolo[2,3-*e*])[1,2,3]triazolo[1,5-*a*]pyrimidine and (indolo[2,3-*e*] and indolo[3,2-*e*])[1,2,3]triazolo[1,5-*a*]pyrimidine.[7–10]

Some of the derivatives belonging to these classes of polycycles were selected for screening tests by the National Cancer Institute (NCI[a]) in the Developmental Therapeutic Program (DTP). In the primary anticancer screening assay, tested against a three-cell line panel consisting of MCF7 (breast), NCI-H460 (lung), and SF-268 (CNS), most of the annelated triazolo-pyrimidines were inactive up to 10^{-4} M concentration. However, considering that, in the case of the antitumor class of actinomycins, the peptide chains play a fundamental role in the DNA interacting capability, we decided to design new series of potential DNA-interactive compounds using, as template for the pharmacofore planar moiety, one of the condensed triazolo-pyrimidine systems in which several side chains can be incorporated. Therefore, we report herein the design, synthesis,

* To whom correspondence should be addressed. Tel.: +39-0916161606. Fax: +39-0916169999. E-mail: almerico@unipa.it.

[a] Abbreviations: NCI, National Cancer Institute; DTP, Developmental Therapeutic Program; CNS, central nervous system; PDB, Protein Data Bank; LGA, Lamarckian genetic algorithm; DMF, *N*,*N*-dimethylformamide; TEA, triethylamine; DCC, dicyclohexylcarbodiimide; DCI, 1,1′-carbonyldiimidazole; DCM, dichloromethane; MG_MID, mean graph midpoint; PCC, Pearson correlation coefficient; 3D-MIND, Drug Discovery and Data Mining Information for New Directions; SOMs, self-organizing maps.

10.1021/jm700964u CCC: $40.75
Published on Web 03/18/2008

Table 1. Selected Side Chain Structures

A	H	**B**	CH_2NH_2
C	$CH_2N(CH_3)_2$	**D**	$CH_2N(CH_2CH_2CH_2CH_3)_2$
E	$CH_2CH_2NH_2$	**F**	$CH_2CH_2N(CH_3)_2$
G	$CH_2CH_2N(CH_2CH_2CH_2CH_3)_2$	**H**	$CH_2CH_2CH_2NH_2$
I	$CH_2CH_2CH_2COOH$	**J**	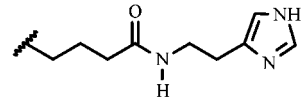
K	$CH_2CH_2CH_2N(CH_2CH_2CH_2CH_3)_2$	**L**	$CH_2CH_2CH_2CONHCH_2COOCH_2CH_3$
M	$CH_2CH_2COOCH_2CH_3$	**N**	$CH_2CH_2CH_2COOCH_2CH_3$
O	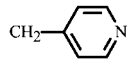	**P**	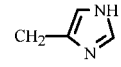
Q	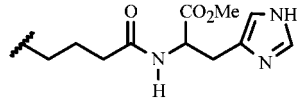	**R**	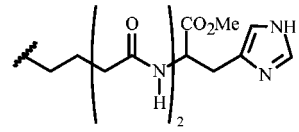
S	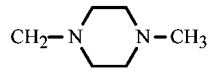	**T**	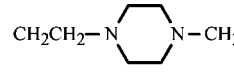
U	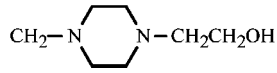	**V**	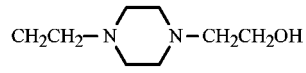

and biological screening results on new 4-substituted indolo[3,2-*e*][1,2,3]triazolo[1,5-*a*]pyrimidine derivatives.

Results and Discussion

Molecular Modeling. First, selected derivatives of the ring system indolo[3,2-*e*][1,2,3]triazolo[1,5-*a*]pyrimidine, compounds **1a**−**e**, were tested by docking experiments. The starting point of all docking calculations is generally the crystal structure of a macromolecule (enzyme, DNA, or RNA fragments and so on), usually obtained from a macromolecule−ligand complex. This complex may be taken from a database of compounds, such as the Cambridge Crystallographic Database[11] or the Protein Data Bank (PDB).[12] The primary consideration in the design of a docking process has to be the development of methods that are both rapid and reasonably accurate.

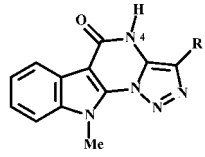

1a-e

a R=CN, b R=$CONH_2$, c R=COOEt, d R=COOMe, e R=Ph

According to the procedure reported in the Experimental Section, our studies were carried out by using the software package AutoDock.[13] This one combines a rapid energy evaluation through precalculated grids of affinity potentials with a variety of search algorithms to find suitable binding positions for a ligand on a given receptor. While the macromolecule is required to be rigid, the program allows torsional flexibility in the ligand. The program searches for the best conformation and for the best place of binding of the ligand within the receptor structure. Several runs of space search were carried out to find the best ligand–receptor binding arrangement. Docking to DNA fragment was performed using the Lamarckian genetic algorithm (LGA)[14] and an empirical binding free energy function, previously tested with success by us in the reconstruction of known DNA−ligand complexes.[15] The PDB was searched for DNA fragments bound with intercalators and the structure 1DSC (an octamer complexed with Actinomycin D) was selected. The original ligand was removed and the DNA sequence was utilized for the docking experiments.

In the case of derivatives **1a**−**e**, the change of free energy of binding was found in the range −11.28 → –13.79 Kcal/mol (cfr Table 2, row A) and is more negative than the value obtained by us, in these calculations, for Actinomycin D (−10.37 kcal/mol). Therefore, these ΔG values calculated for this class of tetracyclic heterocycles demonstrated that, although not being active in the in vitro tests carried out so far, derivatives of this system possessed the electronic and steric feature to interact with DNA and could constitute suitable lead compounds for new anticancer agents. In fact, if they bear suitable side chains in the 4 position of the ring, further interactions of these ligands with DNA minor groove can be envisaged.

At present, relatively little is understood about the mode of action at the molecular level of the majority of minor groove-interacting drugs, although, there is an increasing evidence that they may act by directly blocking or inhibiting protein−DNA recognition. A total of 21 chain shape moieties **B**−**V** of variable length and with different physicochemical character were selected (Table 1). All the related compounds, obtained by the insertion of these chains on the 4 position of derivatives **1a**−**e** were used in the docking calculation to study the types of interaction with DNA.

The predicted binding free energy of the lowest energy docked structure for each ligand considered in this study is reported in Table 2. The calculated ΔG values are in the range

Table 2. Docking Results[a]

	1a	1b	1c	1d	1e	mean
A	−11.28	−12.09	−13.79	−12.66	−13.76	−12.72
B	−12.90	−14.12	−15.51	−14.46	−15.49	−14.50
C	−13.83	−14.39	−15.99	−15.23	−16.40	−15.17
D	−16.32	−16.23	−17.49	−16.58	−18.36	−17.00
E	−12.76	−13.98	−15.59	−15.09	−15.98	−14.68
F	−14.52	−14.35	−15.93	−15.52	−16.07	−15.28
G	−16.42	−15.95	−18.28	−17.21	−17.59	−17.09
H	−12.96	−14.14	−15.64	−15.29	−16.08	−14.82
I	−16.39	−17.62	−18.68	−18.08	−19.04	−17.96
J	−19.52	−20.70	−20.96	−20.44	−20.49	−20.42
K	−18.30	−17.89	−19.95	−18.58	−20.07	−18.96
L	−33.44	−33.91	−36.76	−34.79	−39.68	−35.72
M	−16.47	−16.86	−18.34	−17.31	−18.35	−17.47
N	−17.65	−17.99	−19.57	−16.79	−19.77	−18.35
O	−14.76	−14.92	−16.13	−15.74	−15.96	−15.50
P	−14.65	−14.17	−16.60	−15.83	−16.83	−15.62
Q	−24.99	−27.85	−27.41	−26.95	−26.71	−26.78
R	−26.73	−30.21	−30.96	−28.61	−33.86	−30.07
S	−14.37	−14.93	−16.22	−15.94	−16.73	−15.64
T	−14.51	−15.68	−16.33	−15.49	−15.45	−15.49
U	−17.09	−16.02	−17.00	−18.50	−19.46	−17.61
V	−17.43	−17.15	−18.70	−18.14	−18.07	−17.89
MEAN	−17.15	−17.78	−19.22	−18.37	−19.60	

[a] All energies ($\Delta G_{binding}$) are given in Kcal/mol.

−12.76 → −39.68 Kcal/mol and it is possible to observe a drastic variation of $\Delta G_{binding}$ if compared with the values obtained for the lead compounds **A**. Analyzing the results for the different chains, a regular increase of the binding affinity was generally observed in homologous series for each type of derivative (**a**−**e**) and in the average, compare for example chain **E** and **H** or chain **U** and **V**, for which a mean gain of 0.14–0.18 Kcal/mol was generally evidenced, whereas the effect was more evident in the case of the ester derivatives (0.88 Kcal/mol, chain **M** vs **N**). The same effect was more enhanced if the chain elongation is carried out on the amino end; thus, a net gain of 0.6–0.7 Kcal/mol was observed when switching from the free amino end (chains **B** or **E**) to the methylamino (chains **C** or **F**) up to the dibutylamino compounds (chains **D** or **G**). And, eventually, for these series, the best ligands were found to be those in which both effects were combined, giving rise to compounds presenting the chain **K**, with a net increase in the $\Delta G_{binding}$ values of about 4 Kcal/mol. The influence of the peptido moiety, presenting different acid/basic ends in the side chains, was also investigated (chains **J**, **Q**, **R**, and **L**). It was possible to evidence a general increase in the binding affinity with respect to the derivatives presenting the chain **K**. A histidine end is usually more effective in enhancing the groove interaction (compare for example chain **J** and **Q**), with a net increase of ≈6.4 Kcal/mol in $\Delta G_{binding}$ values. Such an effect became more evident if a bis-peptide (glycine moiety) is introduced to lengthen the chain (compare **Q** and **R** derivatives), for which a $\Delta G_{mean} = -30.07$ Kcal/mol was calculated. However, on the whole, the best chain resulted to be **L** which, combining all the more interesting features above evidenced, conferred to the polycycles of type **1** the highest DNA-binding capability in each case and on the average ($\Delta G_{binding}$ in the range −33.44 → −39.68 Kcal/mol). Thus, as an overall result, among the side chains, **I**, **J**, **K**, **L**, **N**, **Q**, and **R** types conferred to the compounds in which they were incorporated the more negative energy of binding expressed as ΔG_{mean} values. With respect to the nature of the lead compounds, on the average, the one with the highest affinity was demonstrated to be derivative **1e** ($\Delta G_{mean} = -19.60$ Kcal/mol); in this case, the insertion of the above-reported chains generally led to derivatives with a calculated ΔG value more negative than the average one (calculated for the same chain).

In all the cases, the 4-substituted indolo[3,2-*e*][1,2,3]triazolo[1,5-*a*]pyrimidine derivatives were shown to assume a spatial arrangement in which the planar heterocyclic moiety intercalates in GC portion of DNA sequence, whereas the side chain lies close to the minor groove. These findings are exemplified in Figure 1 (right), which shows the DNA-binding mode for the most interesting derivative, presenting the chain **L**, the more efficient in enhancing the DNA binding capability, linked to the phenyl-substituted lead compound **1e**, that has shown the best DNA affinity ($\Delta G_{binding} = -39.68$ Kcal/mol).

Chemistry. With these premises, the synthesis of the compounds, selected on the basis of the molecular modeling results, [**1e**(**I**, **J**, **K**, **L**, **N**, **Q**, **R**)] was successfully achieved through suitable steps, as shown in Scheme 1. The starting tetracycle **1e** was prepared through the classical approach involving the domino reaction between the ethyl 2-azido-1-methyl-1*H*-indole-3-carboxylate and benzylcyanide.[9]

Derivative **1eK** was synthesized in two steps: by reaction of **1e** and 1-bromo-3-chloropropane, the chloro derivative **2** was obtained. This last derivative, upon heating under reflux in dibutylamine *solvent free*, gave **1eK** in good yield.

The majority of compounds bearing the suitable chains were prepared through the key intermediate **1eN**. Thus, this derivative was first obtained from the sodium salt of **1e**, generated in situ by using sodium hydride, and ethyl 4-bromobutyrate in dry DMF, but in very low yield. The use of potassium carbonate (5-fold excess of the starting material), in dry acetonitrile, increased the yields of **1eN** to 70%. Subsequent hydrolysis with NaOH in EtOH/H_2O mixture quantitatively yielded the corresponding carboxylic acid **1eI**.

Derivative **1eL** was synthesized by reacting **1eI** with glycine ethyl ester, in dry dichloromethane and triethylamine (TEA), and using dicyclohexylcarbodiimide (DCC) as coupling agent. Hydrolysis of **1eL** led to the carboxylic acid **3**, which was further reacted with L-histidine methyl ester dihydrochloride, under the above-reported coupling conditions, to give derivative **1eR** in 50% yield.

The amide derivative **1eQ** was obtained from the same key acid **1eI** upon reaction with L-histidine methyl ester dihydrochloride, in dry dichloromethane and TEA, and using DCC as coupling agent.

In all the reactions carried out with DCC, compounds **4** and **5** were isolated and characterized (Scheme 2). To these side products the structure of N-acylureas was assigned, ruling out the isomeric O-acylisoureas **4′** and **5′**, because the treatment of isolated specimen with histidine did not result in any conversion into **1eR** or **1eQ**. These findings resulted in an agreement with the behavior observed by several researchers[16] and with the reactivity of carbodiimides.[17] However, the two N-acylureas were considered as possible DNA binders and, therefore, they were evaluated by docking calculations, showing a binding capability comparable with all the previously selected compounds ($\Delta G_{binding} = -29.05$ Kcal/mol for **4** and −27.07 Kcal/mol for **5**).

Therefore, to avoid the formation of **4** or **5**, the reactions of **3** or **1eI** with L-histidine methyl ester dihydrochloride were carried out in the presence of a different coupling agent (1,1′-carbonyldiimidazole, DCI). By using these experimental conditions, the 4-substituted derivatives were isolated in 70–80% yields.

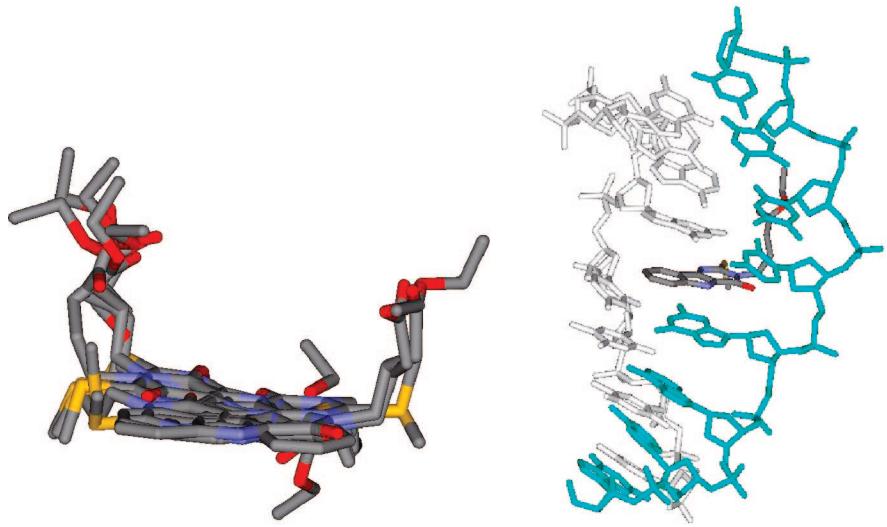

Figure 1. Stick view of 10 superpositioned best scores (left) and best structure docked to DNA fragment (right) for derivative **1eL**.

Scheme 1[a]

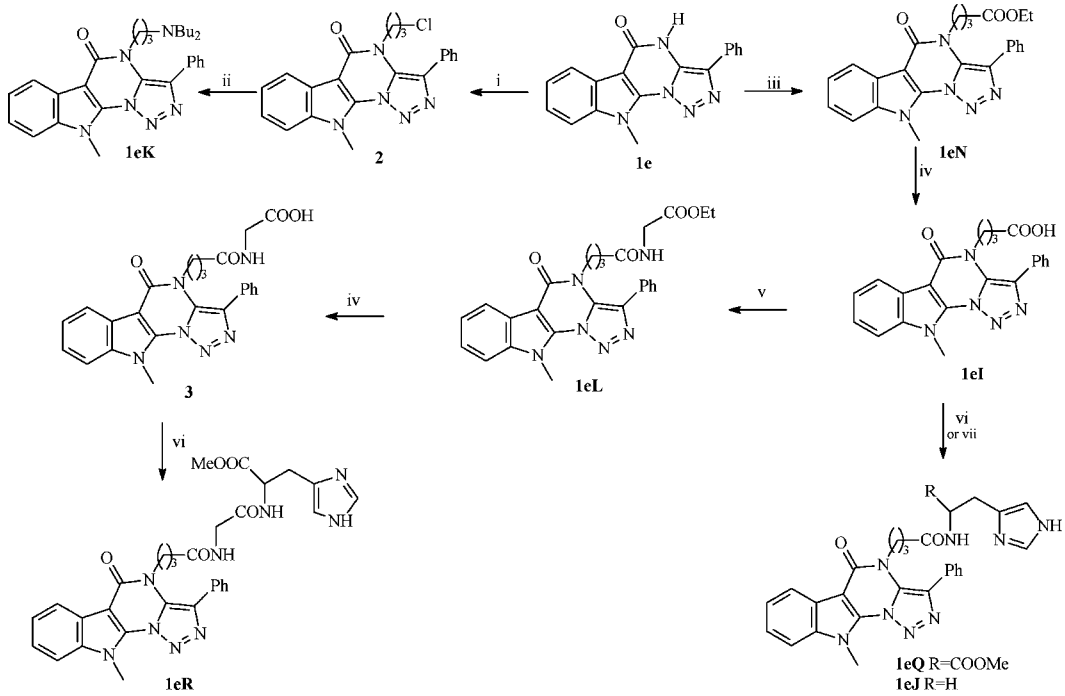

[a] Reagents and conditions: (i) K_2CO_3/MeCN, $Cl(CH_2)_3Br$; (ii) $NHBu_2$; (iii) K_2CO_3/MeCN, ethyl 4-bromobutyrate; (iv) NaOH, EtOH/H_2O; (v) (1) DCC/DCM, 0 °C, (2) glycine ethyl ester hydrochloride/TEA; (vi) (1) DCC/DCM, 0 °C, (2) L-histidine methyl ester dihydrochloride/TEA; (vii) (1) DCI/dioxane, (2) histamine.

Compound **1eJ** was suitably prepared by amidation of the acid **1eI** with histamine, in dioxane, in the presence DCI as coupling agent.

Biological Activity. All the new 4-substituted indolo[3,2-*e*][1,2,3]triazolo[1,5-*a*]pyrimidine derivatives **1e** (**I**, **J**, **K**, **L**, **N**, **Q**, and **R**) and the intermediates **4** and **5** were submitted to the NCI for testing in the DTP.

Three derivatives (**1eN**, **1eI**, and **1eQ**) were tested according to the prescreening procedure against three cell lines, MCF7 (breast), NCI-H460 (lung), and SF-268 (CNS), were found to be inactive at 10^{-4} M concentration (Table 3) and, therefore, were not screened further.

Instead, all the other derivatives **1e** (**J**, **K**, **L**, and **R**) and the N-acylureas **4** and **5** were directly tested against a panel of approximately 60 tumor cell lines that have been grouped in nine disease subpanels, including leukemia, nonsmall-cell lung, colon, central nervous system, melanoma, ovarian, renal, prostate, and breast tumors cell lines (Table 4).

The in vitro test system and the information, encoded by the activity pattern over all cell lines, were obtained (see Experimental Section) according to the previously reported methodology.[18] The antitumor activity of a test compound is given by three parameters for each cell line: pGI_{50} value (GI_{50} is the molar concentration of the compound that inhibits 50% net cell growth), pTGI value (TGI is the molar concentration of the compound leading to total inhibition of net cell growth), and pLC_{50} value (LC_{50} is the molar concentration of the compound that induces 50% net cell death). Moreover, a mean graph midpoint (MG_MID) is calculated for each of the mentioned parameters, giving an average activity parameter over all cell

Scheme 2. Chemical Structures of O-Acylisoureas and N-Acylureas

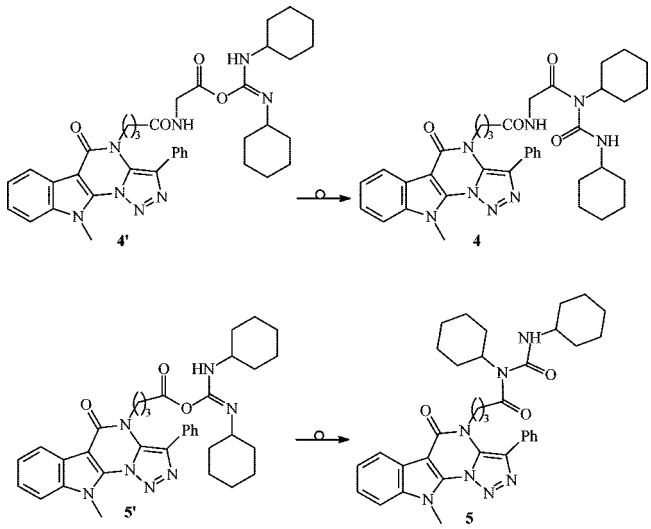

Table 3. Growth Percentage of Tumor Cell Lines[a]

cmpd	MCF7	NCI-H460	SF-268
1eN	114	95	110
1eI	80	95	87
1eQ	116	117	128

[a] Data obtained from NCI's in vitro disease-oriented tumor cell screen.

lines. For the calculation of the MG_MID, insensitive cell lines are included with the highest concentration tested. The discovery of compounds with new selectivity patterns is one of the targets of the screening program. Selectivity of a compound with respect to a certain cell line of the screen is characterized by a high deviation of the particular cell line parameter compared to the MG_MID value.

An evaluation of the data reported in Table 4 revealed that, with the exception of compound **1eR**, active only against the IGROV1 cell line ($pGI_{50} = 4.14$) and PC-3 ($pGI_{50} = 4.52$), all the new synthesized indolo[3,2-*e*][1,2,3]triazolo[1,5-*a*]pyrimidines showed antiproliferative activity against the majority of human tumor cell lines investigated, generally in the low micromolar range. In fact, the number of sensitive cell lines was 39/56 for **1eL**, 49/52 for **4**, 51/55 for **1eK**, and 54/56 for **1eJ** (Table 5), and only in the case of compound **5** the number dropped to 15/59.

Considering the MG_MID values, in the range 4.06−5.04 (Table 5), the most active compound of the series was demonstrated to be derivative **1eJ**, at either GI_{50} and TGI_{50} level (5.04, 4.67; see Supporting Information), and for the number of responding cell lines, followed by **1eL**, **4**, and **1eK**.

With respect to the tumor subpanel, the indolo[3,2-*e*][1,2,3]triazolo[1,5-*a*]pyrimidines resulted particularly effective against all kind of leukemia and, in particular, against the CCRF-CEM cell line (pGI_{50} in the range 4.58−5.82). In fact, the calculated pGI_{50} MG_MID values of leukemia subpanel are always higher than the overall cell lines MG_MID values, with the exception of **1eL**. However, this last showed an excellent response for CNS cancer subpanel. In the case of the most active derivate **1eJ**, it is also evident the good response of all renal subpanel cell lines with an average panel MG_MID value = 5.17, higher than the overall cell lines one, although, the most sensitive cell line resulted to be **HOP-92** of the lung subpanel, with $pGI_{50} = 5.87$.

The inhibition shown by the derivative **1eL** against the CNS subpanel was remarkable, in particular, with respect to the SNB-75 cell line ($pGI_{50} = 5.95$), which was the type of tumor cell line most susceptible to this class of heterocycles. Derivative **1eK** furnished good response toward most of the cell line belonging to the renal subpanel, and especially, in the case of TK-10, for which a $pGI_{50} = 5.72$ was calculated. In the case of the N-acyl-dicyclohexylurea derivatives **4** and **5**, it is possible to evidence that **5** was only specifically active against the majority of CNS and breast cancer lines, although, the higher effect was found against IGROV1 of the ovarian panel ($pGI_{50} = 4.81$), whereas derivative **4** showed a wider range of cytotoxic effects. In this case, it is also necessary to underline an anomalous behavior against SNB-19 (CNS cancer) and SK-OV-3 (ovarian cancer) for which a strong inhibitory effect was evidenced at micromolar concentrations, although, it was not possible to quantify the pGI_{50} value according to the standard NCI procedure.

When valuating this class of compounds with respect to the MG_MID values at TGI and LC_{50} level (Table 6), again derivative **1eJ** was demonstrated to be the most active as far as the MG_MID values are concerned, although, the renal and CNS subpanel cell lines resulted sensitive for compound **1eL**, as evidenced by the panel MG_MID values (4.68 and 4.82, respectively) higher than the overall cell lines one. It is also of remarkable interest the low number of cell lines giving positive LC_{50} in the case of **1eL** and **4**, a result that can give account of the low toxicity of such compounds.

With respect to Dactinomycin (our starting reference drug),[19] the series of 4-substituted indolo-triazolo-pyrimidines resulted less potent, but our more interesting compounds, **1eJ** and **1eL**, showed selectivity with respect to renal and CNS subpanel cell lines against which Dactinomycin was not particularly effective.

To predict the mechanism of action, the computerized analysis COMPARE[20] was performed on the most active derivative **1eJ** (MG_MID $pGI_{50} = 5.04$). Tested as seed against the NCI "Standard Agents" database, it showed a Pearson correlation coefficient (PCC) of 0.551 at GI_{50} level and a lower value at TGI level (0.542). In all the cases, the first rank was with Acodazole (NSC305884), a typical intercalating agent.

We also utilized the facility 3D-MIND (Drug Discovery and Data Mining Information for New Directions)[21] tools that allows a simultaneous examination of the information found in the DTP antitumor drug screen by using "self-organizing maps" (SOMs), which cluster this data in the high-dimensional GI_{50} space and provide a means of its visual translation into a two-dimensional anticancer map. SOM anticancer maps organize the data from tested agents into regions, which share the same pattern of growth inhibition and which substantially reflect their molecular targets and modes of action. The Projected Cluster List gives the NSC number and the location corresponding to the projected compound. The results of this analysis on our derivative indicate its location in the N2 region map, related to membrane integrity. Moreover, by analyzing the mechanism of action map, **1eJ** was found located between the cytidine analogues and the anthracyclines and, in particular, in the region in which the 1,4-bis[[2-[(2-aminoethyl)amino]ethyl]amino]-5,8-dihydroxy-9,10-anthracenedione (NSC660224) is found.

These results, together with the low value of the PCC in the COMPARE analysis, could suggest that this new class of compounds may have a mechanism of action that could be related to that of pure intercalating drugs, although, the behavior as antimetabolite agents can not be excluded. We suppose that both the planar chromophore and the side chain are fundamental for the interaction with DNA and that this interaction may help

Table 4. Inhibition of In Vitro Cancer Cell Lines by 4-Substituted Indolo-triazolo-pyrimidines[a]

	pGI$_{50}$[b]							pGI$_{50}$[b]					
panel/cell line	**1eJ**	**1eL**	**4**	**1eK**	**5**	**1eR**	panel/cell line	**1eJ**	**1eL**	**4**	**1eK**	**5**	**1eR**
			Leukemia							Melanoma			
CCRF-CEM	5.82	4.58	5.08	5.38	<4.00	<4.00	SK-MEL-2	4.99	5.02	4.48	<4.00	<4.00	<4.00
HL-60(TB)	4.93	4.69	5.54	5.59	<4.00	<4.00	SK-MEL-28	5.05	<4.30	nd	<4.00	<4.00	<4.00
K-562	5.05	5.33	4.64	4.86	<4.00	<4.00	SK-MEL-5	5.04	nd	5.22	4.50	<4.00	<4.00
MOLT-4	5.40	<4.30	4.84	4.86	<4.00	<4.00	UACC-257	4.92	<4.30	4.18	4.54	<4.00	<4.00
RPMI-8226	4.98	4.97	5.37	5.22	<4.00	<4.00	UACC-62	5.01	5.14	4.59	4.65	<4.00	<4.00
SR	5.39	nd[c]	5.52	nd	<4.00	<4.00				Ovarian Cancer			
			Non-Small Cell Lung Cancer				IGROV1	nd	5.05	5.55	nd	4.81	4.14
A549/ATCC	4.89	4.48	4.42	4.36	<4.00	<4.00	OVCAR-3	5.08	4.90	4.71	4.31	<4.00	<4.00
EKVX	5.00	4.69	nd	4.25	<4.00	<4.00	OVCAR-4	4.99	<4.30	nd	4.76	4.42	<4.00
HOP-62	5.12	5.23	4.82	4.51	<4.00	<4.00	OVCAR-5	4.96	4.56	4.81	4.65	<4.00	<4.00
HOP-92	5.87	5.44	nd	4.73	<4.00	<4.00	OVCAR-8	5.00	4.60	5.13	4.40	<4.00	<4.00
NCI-H226	<4.30	4.60	4.40	4.24	<4.00	<4.00	SK-OV-3	4.99	5.17	nc	4.52	<4.00	<4.00
NCI-H23	4.88	4.93	4.81	4.89	<4.00	<4.00				Renal Cancer			
NCI-H322M	4.96	<4.30	<4.00	4.54	<4.00	<4.00	786–0	5.66	5.29	4.73	4.41	<4.00	<4.00
NCI-H460	4.96	<4.30	4.49	4.39	<4.00	<4.00	A498	5.12	5.14	4.51	4.37	4.18	<4.00
NCI-H522	nd	5.19	4.80	nd	4.16	<4.00	ACHN	5.01	5.03	4.58	4.46	<4.00	<4.00
			Colon Cancer				CAKI-1	4.92	5.08	4.49	4.30	<4.00	<4.00
COLO 205	5.07	<4.30	5.55	5.30	<4.00	<4.00	RXF 393	5.13	5.88	4.96	4.85	4.20	<4.00
HCC-2998	5.02	<4.30	4.99	4.69	<4.00	<4.00	SN12C	5.06	<4.30	4.71	4.71	<4.00	<4.00
HCT-116	5.23	5.04	4.85	4.73	4.04	<4.00	TK-10	5.32	5.06	<4.00	5.72	<4.00	<4.00
HCT-15	4.84	<4.30	4.97	4.68	<4.00	<4.00	UO-31	5.13	4.32	4.50	5.22	<4.00	<4.00
HT-29	5.07	<4.30	nd	5.11	<4.00	<4.00				CNS Cancer			
KM12	5.09	<4.30	4.50	4.47	<4.00	<4.00	PC-3	5.05	5.07	4.64	4.74	<4.00	4.52
SW-620	4.89	<4.30	5.42	4.58	<4.00	<4.00	DU-145	5.16	4.49	4.73	4.32	<4.00	<4.00
			CNS Cancer							Breast Cancer			
SF-268	4.93	4.85	4.82	<4.00	4.01	<4.00	MCF7	4.89	4.50	5.44	4.43	4.19	<4.00
SF-295	5.04	5.32	<4.00	4.50	4.10	<4.00	NCI/ADR-RES	<4.30	<4.30	4.81	4.85	4.02	<4.00
SF-539	5.03	5.37	4.70	4.18	4.42	<4.00	MDA-MB-231/ATCC	5.03	4.83	4.91	4.44	4.14	<4.00
SNB-19	4.93	5.23	nc[d]	<4.00	<4.00	<4.00	HS 578T	4.98	5.35	5.03	4.40	<4.00	<4.00
SNB-75	4.98	5.95	nd	4.82	4.35	<4.00	MDA-MB-435	4.99	<4.30	4.60	4.41	<4.00	<4.00
U251	5.02	5.38	4.91	4.48	<4.00	<4.00	T-47D	4.98	4.36	nd	4.26	4.25	<4.00
			Melanoma				BT-549	nd	nd	4.57	nd	4.14	<4.00
LOX IMVI	4.95	4.60	4.88	4.55	<4.00	<4.00							
MALME-3M	5.12	<4.30	4.33	4.55	<4.00	<4.00	MG_MID[e]	5.04	4.79	4.78	4.61	4.06	4.01
M14	4.92	4.73	4.51	4.67	<4.00	<4.00							

[a] Data obtained from NCI's in vitro disease-oriented tumor cells screen. [b] pGI$_{50}$ is the –log of the molar concentration causing 50% growth inhibition of tumor cells. [c] Not determined. [d] Not calculated. [e] MG_MID = mean graph midpoint = arithmetical mean value for all tested cancer cell lines. If the indicated effect was not attainable within the used concentration interval, the highest tested concentration was used for the calculation.

Table 5. Overview of the Results (pGI$_{50}$) of the In Vitro Antitumor Screening for Indolo-triazolo-pyrimidines[a]

cmpd	# cell lines investigated	# cell lines giving positive pGI$_{50}$	pGI$_{50}$[b] range	MG_MID[c]
5	59	15	4.81–4.01	4.06
1eK	55	51	5.72–4.18	4.61
4	52	49	5.55–4.18	4.78
1eL	56	39	5.95–4.32	4.79
1eJ	56	54	5.87–4.84	5.04

[a] Data obtained from the NCI's in vitro disease-oriented human tumor cells screen. [b] pGI$_{50}$ is the −log of the molar concentration that inhibits 50% net cell growth. [c] MG_MID = mean graph midpoint = arithmetical mean value for all tested cancer cell lines. If the indicated effect was not attainable within the used concentration interval, the highest tested concentration was used for the calculation.

position drug molecules on DNA for other reaction responsible of the cytotoxic and antitumor activity of these compounds.

Conclusions

In conclusion, this class of compounds combines two of the main features of DNA-interactive drugs and a very tight DNA-binding capability has to be expected, as suggested by our docking studies. The molecular modeling results correlate well with the experimental activity data and the choice of suitable chains can be theoretically supported: a more negative $\Delta G_{binding}$ value is mirrored by a higher inhibitory activity. The class of 4-substituted indolo[3,2-*e*][1,2,3]triazolo[1,5-*a*]pyrimidines studied herein represents an improvement of the original lead compounds worthy of further development. Because the COMPARE analysis and 3D-MIND tools revealed a mechanism of action strictly related to that of DNA-interacting drugs, but not ruled out alternative ones, the investigation and discovery of the exact mechanism can constitute a decisive step toward the optimization of the antitumor activity.

Experimental Section

Molecular Modeling. Ligand Setup. The 3D structures of the ligands were constructed, preoptimized with implemented MM2 force field, and further refined using Vega 1.5.[22] The PM3 method was used for geometry optimization and charge calculation. To allow flexibility in the ligand, it is necessary to assign the routable bonds; in our case, all the rotamers were allowed.

DNA Fragment Setup. The PDB file of the selected structure 1DSC was downloaded from the database and the ligand was removed from the fragment. The resulting macromolecule was setup for docking as follows: polar hydrogens were added using the PROTONATE utility. Solvation parameters were added to the final protein file using the ADDSOL utility.

The grid maps representing the protein in the actual docking process were calculated with AutoGrid. The grids (one for each atom type in the ligand, plus one for electrostatic interactions) were chosen to be sufficiently large to include not only the active site but also significant portions of the surrounding surface. The points of the grids were thus 60 × 60 × 60, with a grid spacing of 0.375 Å.

Docking. Docking of the ligands into receptor was carried out using AutoDock (version 3.0.5) set of programs.[23] It was carried

Table 6. Overview of the Results (pTGI and pLC_{50}) of the In Vitro Antitumor Screening for Indolo-triazolo-pyrimidines[a]

cmpd	# cell lines investigated	# cell lines giving positive pTGI	pTGI[b] range	MG_MID[d]	# cell lines investigated	# cell lines giving positive pLC_{50}	pLC_{50}[c] range	MG_MID
1eK	56	19	4.97−4.02	4.09				
4	51	21	5.29−4.01	4.18	52	7	5.07−4.01	4.03
1eL	56	22	5.45−4.31	4.46	56	5	4.77−4.32	4.32
1eJ	56	52	5.26−4.33	4.67	56	38	4.57−4.31	4.39

[a] Data obtained from the NCI's in vitro disease-oriented human tumor cells screen. [b] pTGI is the −log of the molar concentration giving total growth inhibition. [c] pLC_{50} is the −log of the molar concentration leading to 50% net cell death. [d] MG_MID = mean graph midpoint = arithmetical mean value for all tested cancer cell lines. If the indicated effect was not attainable within the used concentration interval, the highest tested concentration was used for the calculation.

out using the empirical free energy function and the Lamarckian genetic algorithm,[14] applying a standard protocol, with an initial population of 100 randomly placed individuals, a maximum number of 1.5×10^6 energy evaluations, a mutation rate of 0.02, a crossover rate of 0.80, and an elitism value of 1. Proportional selection was used, where the average of the worst energy was calculated over a window of the previous 10 generations. For the local search, the so-called pseudo-Solis and Wets algorithm[24] was applied using a maximum of 300 iterations per local search. The probability of performing local search on an individual in the population was 0.06, and the maximum number of consecutive successes or failures before doubling or halving the local search step size was 4. A total of 10 independent docking runs were carried out for each ligand. At the end of each AutoDock execution, in which more than one run was performed, the program outputs a list of clusters and their energies. The clustering of docked conformations is determined by the tolerance specified in Å. In our cases, the results differing by less than 1.0 Å in positional root-mean-square deviation (rmsd) were clustered together and represented by the result with the most favorable free energy of binding. The best representative from each cluster (the one with the lowest energy) is written out in PDBQ format at the end of the log file. These structures can be read into any appropriate molecular modeling system. The table of ranked clusters shows the final docked energy for each conformation and the rms difference between the lowest energy member of the group and every other member. The rms for the lowest member of the group is by definition zero. After this table, the structures are output in PDBQ format. Each conformation has a set of remark records, one of which describes the rms difference between itself and the coordinates specified in the original input PDBQ file.

Chemistry. All melting points were taken on a Buchi-Tottoli capillary apparatus and are uncorrected; IR spectra were determined in bromoform with a Jasco FT/IR 5300 spectrophotometer; ^{1}H and ^{13}C NMR spectra were measured in DMSO-d_6 solution (TMS as internal reference) at 200 and 50.3 MHz, respectively, using a Bruker AC-E series 200 MHz spectrometer. ^{13}C NMR spectra are reported, indicating the multiplicity, (s, singlet; d, doublet; t, triplet; q, quartet) assigned by DEPT135 experiments. Column chromatography was performed with Merck silica gel 230–400 mesh ASTM or with a Biotage FLASH40i chromatography module (prepacked cartridge system). Microanalyses were in agreement with theoretical values ±0.4%.

4-(3-Chloropropyl)-10-methyl-3-phenyl-4*H*-indolo[3,2-*e*][1,2,3]-triazolo[1,5-*a*]pyrimidin-5(10*H*)-one (2). To a stirred suspension of **1e**[9] (0.5 g, 1.6 mmol) in dry acetonitrile (20 mL), potassium carbonate (0.66 g, 4.8 mmol) and 1-bromo-3-chloropropane (0.47 mL, 4.8 mmol) were added. The mixture was heated at reflux for 5 h, cooled to room temperature, and evaporated under reduced pressure. The residue was purified by column chromatography using dichloromethane as eluant to afford compound **2** as a white solid (0.44 g, 1.12 mmol). Yield 70%, mp 202 °C. IR: 1687 (*C*═O) cm^{-1}. ^{1}H NMR ppm: 8.28 (d, J = 7.4 Hz, 2H, H-2′ and H-6′); 8.08 (d, J = 7.4 Hz, 1H, H-6); 7.62–7.31 (m, 6H, H-7, H-8, H-9, H-3′, H-4′ and H-5′); 5.11 (t, J = 7.3 Hz, 2H, NCH_2); 3.92 (s, 3H, NCH_3); 3.72 (t, J = 5.9 Hz, 2H, CH_2Cl); 2.30–2.24 (m, 2H, $CH_2\underline{CH_2}CH_2$). ^{13}C NMR ppm: 156.0 (s); 151.2 (s); 144.5 (s); 138.1 (s); 135.1 (s); 129.5 (d); 128.8 (d); 128.6 (s); 126.3 (d); 124.5 (d); 121.3 (d); 121.1 (s); 120.3 (d); 109.6 (d); 94.6 (s); 53.2 (t); 42.1 (t); 30.8 (t); 27.9 (q).

4-[3-(Dibutylamino)propyl]-10-methyl-3-phenyl-4*H*-indolo[3,2-*e*][1,2,3]triazolo[1,5-*a*]pyrimidin-5(10*H*)-one (1eK). A stirred suspension of **2** (0.5 g, 1.28 mmol) in dibutylamine (20 mL) was heated at reflux for 5 h. After cooling water (10 mL) was added and the mixture was carefully adjusted to pH = 7 with 6 M hydrochloric acid, extracted with dichloromethane, dried over sodium sulfate, and evaporated to dryness. The residue was purified by flash chromatography using ethyl acetate as eluant to afford compound **1eK** as a white solid (0.43 g, 0.89 mmol). Yield 70%, mp 205 °C. IR: 1656 (*C*═O) cm^{-1}. ^{1}H NMR ppm: 8.48 (d, J = 7.4 Hz, 2H, H-2′ and H-6′); 8.07 (d, J = 7.4 Hz, 1H, H-6); 7.60–7.30 (m, 6H, H-7, H-8, H-9, H-3′, H-4′ and H-5′); 5.03 (t, J = 6.6 Hz, 2H, $CON\underline{CH_2}CH_2CH_2N$); 3.90 (s, 3H, NCH_3); 2.39 (t, J = 7.4 Hz, 2H, $NCH_2CH_2\underline{CH_2}N$); 2.27–2.24 (m, 4H, 2 × $N\underline{CH_2}CH_2CH_2CH_3$); 1.86–1.83 (m, 2H, $CONCH_2\underline{CH_2}CH_2N$); 1.23–1.20 (m, 8H, 2 × $NCH_2\underline{CH_2CH_2}CH_3$); 0.80–0.75 (m, 6H, 2 × $NCH_2CH_2CH_2\underline{CH_3}$). ^{13}C NMR ppm: 154.6 (s); 151.6 (s); 144.8 (s); 138.3 (s); 130.9 (s); 129.7 (d); 128.9 (d); 128.6 (s); 126.3 (d); 124.7 (d); 121.4 (d); 121.1 (s); 120.3 (d); 109.8 (d); 94.6 (s); 53.7 (t); 52.4 (t); 49.6 (t); 28.0 (q); 26.9 (t); 19.7 (t); 13.6 (q).

Ethyl 4-(10-Methyl-3-phenyl-5-oxo-5,10-dihydro-4*H*-indolo[3,2-*e*][1,2,3]triazolo[1,5-*a*]pyrimidin-4-yl)butanoate (1eN). To a stirred suspension of **1e**[9] (0.5 g, 1.6 mmol) in dry acetonitrile, (20 mL) potassium carbonate (1.09 g, 7.9 mmol) and ethyl 4-bromobutyrate (1.13 mL, 7.9 mmol) were added. The mixture was heated at reflux for 5 h, cooled to room temperature, and evaporated under reduced pressure. The residue was purified by column chromatography using dichlorometane as eluant to afford compound **1eN** as a white solid (0.48 g, 1.12 mmol.). Yield 70%, mp 128.9 °C. IR: 1729 (*C*═O), 1691 (*C*═O) cm^{-1}. ^{1}H NMR ppm: 8.45 (d, J = 7.4 Hz, 2H, H-2′ and H-6′); 8.05 (d, J = 7.4 Hz, 1H, H-6); 7.63–7.29 (m, 6H, H-7, H-8, H-9, H-3′, H-4′ and H-5′); 5.03 (t, J = 6.6 Hz, 2H, NCH_2); 3.97–3.88 (m, 5H, NCH_3 and $O\underline{CH_2}CH_3$); 2.38 (t, J = 7.4 Hz, 2H, $\underline{CH_2}CO$); 2.07–1.99 (m, 2H, $CH_2\underline{CH_2}CH_2$); 1.06 (t, J = 7.3 Hz, 3H, $OCH_2\underline{CH_3}$). ^{13}C NMR ppm: 171.9 (s); 154.4 (s); 151.3 (s); 144.5 (s); 138.1 (s); 136.1 (s); 129.4 (d); 128.7 (d); 128.6 (s); 126.1 (d); 124.4 (d); 121.2 (d); 121.1 (s); 120.2 (d); 109.5 (d); 94.6 (s); 59.8 (t); 55.0 (t); 30.4 (t); 27.9 (q); 23.5 (t); 13.8 (q).

4-(10-Methyl-3-phenyl-5-oxo-5,10-dihydro-4*H*-indolo[3,2-*e*][1,2,3]triazolo[1,5-*a*]pyrimidin-4-yl)butanoic Acid (1eI). To a stirred suspension of **1eN** (0.5 g, 1.16 mmol) in dry ethanol (10 mL), a solution of sodium hydroxide (0.23 g, 5.8 mmol) in water (10 mL) was added dropwise. The mixture was heated at reflux for 1 h until a clear solution was obtained. The ethanol was evaporated under reduced pressure and the aqueous layer was then carefully adjusted to pH =1 with 6 M hydrochloric acid. The resulting solid was filtered off, air-dried, and recrystallized from ethanol to afford compound **1eI** as a colorless solid (0.46 g, 1.16 mmol). Yield 100%, mp 219.3 °C. IR: 3519–2900 (OH), 1716 (*C*═O), 1681 (*C*═O) cm^{-1}. ^{1}H NMR ppm: 8.47 (d, J = 7.3 Hz, 2H, H-2′ and H-6′); 8.07 (d, J = 7.3 Hz, 1H, H-6); 7.66–7.28 (m, 7H, H-7, H-8, H-9, H-3′, H-4′, H-5′ and OH); 5.02 (t, J = 5.9 Hz, 2H, NCH_2); 3.89 (s, 3H, NCH_3); 2.32 (t, J = 7.4 Hz, 2H, $\underline{CH_2}CO$); 2.08–1.94 (m, 2H, $CH_2\underline{CH_2}CH_2$). ^{13}C NMR ppm: 173.6 (s); 154.5 (s); 151.4 (s); 144.6 (s); 138.2 (s); 136.2 (s); 129.5 (d); 128.9 (d); 128.7 (s); 126.2 (d); 124.6 (d); 121.3 (d); 121.2 (s); 120.3 (d); 109.6 (d); 94.7 (s); 55.2 (t); 30.6 (t); 27.9 (q); 23.6 (t).

**Ethyl *N*-[4-(10-Methyl-3-phenyl-5-oxo-5,10-dihydro-4*H*-indolo[3,2-*e*][1,2,3]triazolo[1,5-*a*]pyrimidin-4-yl)butanoyl]glyci-

nate (1eL). To a stirred suspension of carboxylic acid **1eI** (0.5 g, 1.25 mmol) in dry dichloromethane (10 mL), cooled to 0 °C, DCC (0.26 g, 1.25 mmol) and triethylamine (0.17 mL, 1.25 mmol) were added. After 2 h, glycine ethyl ester hydrochloride (0.17 g, 1.25 mmol) was added and the mixture was stirred for further 5 h at room temperature. Evaporation of the solvent under reduced pressure gave a solid that was purified by column chromatography. Using dichloromethane as eluant, compound **5** (<5% yield) was isolated. Elution with dichloromethane/ethyl acetate 9:1 gave compound **1eL** as a white solid (0.30 g, 0.63 mmol). Yield 50%, mp 217 °C. IR: 3322 (NH), 1752 (*C*═O), 1693 (*C*═O), 1650 (*C*═O) cm^{-1}. ^1H NMR ppm: 8.47 (d, $J = 7.3$ Hz, 2H, H-2′ and H-6′); 8.15 (t, $J = 5.1$ Hz, 1H, NHCH$_2$); 8.07 (d, $J = 7.3$ Hz, 1H, H-6); 7.64–7.26 (m, 6H, H-7, H-8, H-9, H-3′, H-4′ and H-5′); 5.01 (t, $J = 6.6$ Hz, 2H, NCH$_2$); 4.07 (q, $J = 7.3$ Hz, 2H, OCH$_2$CH$_3$); 3.89 (s, 3H, NCH$_3$); 3.61 (d, $J = 5.1$ Hz, 2H, NHCH$_2$CO); 2.22 (t, $J = 7.3$ Hz, 2H, CH$_2$CO); 2.02–1.96 (m, 2H, CH$_2$CH$_2$CH$_2$); 1.06 (t, $J = 7.3$ Hz, 3H, OCH$_2$CH$_3$). ^{13}C NMR ppm: 173.6 (s); 171.2 (s); 154.5 (s); 151.4 (s); 144.6 (s); 138.2 (s); 136.2 (s); 129.5 (d); 128.9 (d); 128.7 (s); 126.2 (d); 124.6 (d); 121.3 (d); 121.2 (s); 120.3 (d); 109.6 (d); 94.7 (s); 55.2 (t); 55.0 (t); 41.6 (t); 30.6 (t); 27.9 (q); 23.6 (t); 13.8 (t).

***N*-[4-(10-Methyl-3-phenyl-5-oxo-5,10-dihydro-4*H*-indolo[3,2-*e*][1,2,3]triazolo[1,5-*a*]pyrimidin-4-yl)butanoyl]glycine (3).** To a stirred suspension of **1eL** (0.5 g, 1.02 mmol) in dry ethanol (10 mL), a solution of sodium hydroxide (0.2 g, 5.1 mmol) in water (10 mL) was added dropwise. The mixture was incubated at 50 °C for 3 h until a clear solution was obtained. The ethanol was evaporated under reduced pressure and the aqueous layer was then carefully adjusted to pH = 1 with 6 M hydrochloric acid. The resulting solid was filtered off, air-dried, and recrystallized from ethanol to afford compound **3** as a white solid (0.47 g, 1.02 mmol). Yield 100%, mp 215 °C. IR: 3446–2900 (OH and NH), 1731 (*C*═O), 1666 (*C*═O) cm^{-1}. ^1H NMR ppm: 8.47 (d, $J = 7.3$ Hz, 2H, H-2′ and H-6′); 8.15 (t, 1H, $J = 5.1$ Hz, NH); 8.07 (d, $J = 7.3$ Hz, 1H, H-6); 7.66–7.28 (m, 6H, H-7, H-8, H-9, H-3′, H-4′ and H-5′); 5.02 (t, $J = 6.6$ Hz, 2H, NCH$_2$CH$_2$CH$_2$) 3.89 (s, 3H, NCH$_3$); 3.61 (d, 2H, $J = 5.1$ Hz, NHCH$_2$CO); 2.32 (t, $J = 7.4$ Hz, 2H, CH$_2$CH$_2$CH$_2$CO); 2.04–1.99 (m, 2H, CH$_2$CH$_2$CH$_2$). ^{13}C NMR ppm: 173.6 (s); 171.2 (s); 154.5 (s); 151.4 (s); 144.6 (s); 138.2 (s); 136.2 (s); 129.5 (d); 128.9 (d); 128.7 (s); 126.2 (d); 124.6 (d); 121.3 (d); 121.2 (s); 120.3 (d); 109.6 (d); 94.7 (s); 55.2 (t); 41.6 (t); 30.6 (t); 27.9 (q); 23.6 (t).

Methyl *N*-[4-(10-Methyl-3-phenyl-5-oxo-5,10-dihydro-4*H*-indolo[3,2-*e*][1,2,3]triazolo[1,5-*a*]pyrimidin-4-yl)butanoyl]glycinhistidinate (1eR) and *N*-(2-{Cyclohexyl[(cyclohexylamino)-carbonyl]amino}-2-oxoethyl)-4-(10-methyl-3-phenyl-5-oxo-5,10-dihydro-4*H*-indolo[3,2-*e*][1,2,3]triazolo[1,5-*a*]pyrimidin-4-yl)butanamide (4). To a stirred suspension of **3** (0.5 g, 1.09 mmol) in dry dichloromethane (10 mL), cooled to 0 °C, DCC (0.22 g, 1.09 mmol) and triethylamine (0.15 mL, 1.09 mmol) were added. After 2 h, L-histidine methyl ester dihydrochloride (0.26 g, 1.09 mmol) was added, and the mixture was stirred for further 24 h at room temperature. Evaporation of the solvent under reduced pressure gave a solid that was purified by column chromatography. Using dichloromethane as eluant compound **4** as a colorless solid (0.16 g, 0.24 mmol) was isolated. Yield 22%, mp 152 °C. IR: 3324 (NH), 2929 (NH), 1691 (*C*═O), 1652 (*C*═O) cm^{-1}. ^1H NMR ppm: 8.54 (d, $J = 7.4$ Hz, 2H, H-2′ and H-6′); 8.32 (t, $J = 5.1$ Hz, 1H, NHCH$_2$); 8.09 (d, $J = 7.4$ Hz, 1H, H-6); 7.60–7.34 (m, 6H, H-7, H-8, H-9, H-3′, H-4′ and H-5′); 5.59 (d, $J = 7.3$ Hz, 1H, NH); 5.05 (t, $J = 6.6$ Hz, 2H, NCH$_2$); 3.95 (s, 3H, NCH$_3$); 3.82 (d, $J = 5.1$ Hz, 2H, NHCH$_2$CO); 2.24 (t, $J = 7.4$ Hz, 2H, CH$_2$CO); 2.04–1.97 (m, 2H, CH$_2$CH$_2$CH$_2$); 1.70–1.24 (m, 22H, 2 × Cy).

Further elution with dichloromethane/methanol 9:1 gave compound **1eR** as a colorless solid (0.33 g, 0.54 mmol). Yield 50%, mp 147 °C. IR: 3313 (NH), 2948 (NH), 1737 (*C*═O), 1685 (*C*═O) cm^{-1}. ^1H NMR ppm: 8.47 (d, $J = 7.3$ Hz, 2H, H-2′ and H-6′); 8.28 (d, $J = 7.4$ Hz, 1H, NHCH); 8.15 (t, $J = 5.1$ Hz, 1H, NHCH$_2$); 8.07 (d, $J = 7.3$ Hz, 1H, H-6); 7.64–7.26 (m, 7H, H-7, H-8, H-9, H-3′, H-4′, H-5′ and H-2″); 6.79 (s, 1H, H-5″); 5.01 (t, $J = 6.6$ Hz, 2H, NCH$_2$); 4.43 (m, 1H, CH); 3.89 (s, 3H, NCH$_3$); 3.61 (d, $J = 5.1$ Hz, 2H, NHCH$_2$CO); 3.56 (s, 3H, OCH$_3$); 2.86 (d, $J = 5.1$ Hz, 2H, CHCH$_2$); 2.22 (t, $J = 7.3$ Hz, 2H, CH$_2$CO); 2.02–1.96 (m, 2H, CH$_2$CH$_2$CH$_2$). ^{13}C NMR ppm: 171.5 (s); 171.3 (s); 169.0 (s); 154.0 (s); 151.4 (s); 144.5 (s); 138.1 (s); 136.2 (s); 134.8 (d); 131.3 (s); 129.4 (d); 128.8 (d); 128.6 (s); 126.2 (d); 124.5 (d); 121.2 (d); 121.1 (s); 120.2 (d); 116.6 (d); 109.5 (d); 94.7 (s); 55.4 (t); 52.3 (d); 51.8 (q); 41.6 (t); 31.8 (t); 27.9 (q); 27.4 (t); 24.1 (t).

Methyl *N*-[4-(10-Methyl-3-phenyl-5-oxo-5,10-dihydro-4*H*-indolo[3,2-*e*][1,2,3]triazolo[1,5-*a*]pyrimidin-4-yl)butanoyl]histidinate (1eQ) and *N*-Cyclohexyl-*N*-[(cyclohexylamino)carbonyl]4-(10-methyl-3-phenyl-5-oxo-5,10-dihydro-4*H*-indolo[3,2-*e*][1,2,3]triazolo[1,5-*a*]pyrimidin-4-yl)butanamide (5). To a stirred suspension of carboxylic acid **1eI** (0.5 g, 1.25 mmol) in dry dichloromethane (10 mL), cooled to 0 °C, DCC (0.26 g, 1.25 mmol) and triethylamine (0.17 mL, 1.25 mmol) were added. After 2 h, L-histidine methyl ester dihydrochloride (0.3 g, 1.25 mmol) was added and the mixture was stirred for an additional 24 h at room temperature. Evaporation of the solvent under reduced pressure gave a solid that was purified by column chromatography. Using dichloromethane as eluant compound **5** (0.16 g, 0.27 mmol) was isolated. Yield 22%, mp 215.9 °C. IR: 3326 (NH), 1677 (*C*═O), 1652 (*C*═O) cm^{-1}. ^1H NMR ppm: 8.48 (d, $J = 7.4$ Hz, 2H, H-2′ and H-6′); 8.08 (d, $J = 7.4$ Hz, 1H, H-6); 7.61–7.29 (m, 6H, H-7, H-8, H-9, H-3′, H-4′ and H-5′); 5.58 (d, $J = 7.3$ Hz, 1H, NH); 5.05 (t, $J = 6.6$ Hz, 2H, NCH$_2$); 3.92 (s, 3H, NCH$_3$); 2.31 (t, $J = 7.4$ Hz, 2H, CH$_2$CO); 2.05–2.02 (m, 2H, CH$_2$CH$_2$CH$_2$); 1.70–1.06 (m, 22H, 2 × Cy).

Further elution with dichloromethane/methanol 9:1 gave compound **1eQ** (0.35 g, 0.63 mmol). Yield 50%, mp 187 °C. IR: 3342 (NH), 1737 (*C*═O), 1691 (*C*═O), 1656 (*C*═O) cm^{-1}. ^1H NMR ppm: 8.46 (d, $J = 7.4$ Hz, 2H, H-2′ and H-6′); 8.29 (d, $J = 7.3$ Hz, 1H, NH); 8.05 (d, $J = 7.4$ Hz, 1H, H-6); 7.60–7.29 (m, 7H, H-7, H-8, H-9, H-3′, H-4′, H-5′ and H-2″); 6.77 (s, 1H, H-5″); 4.96 (t, $J = 6.6$ Hz, 2H, NCH$_2$); 4.44 (m, 1H, CH); 3.88 (s, 3H, NCH$_3$); 3.56 (s, 3H, OCH$_3$); 2.83 (d, $J = 7.4$ Hz, 2H, CHCH$_2$); 2.20 (t, $J = 7.4$ Hz, 2H, CH$_2$CO); 2.06–1.96 (m, 2H, CH$_2$CH$_2$CH$_2$). ^{13}C NMR ppm: 172.1 (s); 171.2 (s); 154.4 (s); 151.4 (s); 144.6 (s); 138.1 (s); 136.2 (s); 134.9 (d); 133.1 (s); 129.5 (d); 128.9 (d); 128.7 (s); 126.2 (d); 124.5 (d); 121.3 (d); 121.1 (s); 120.3 (d); 116.6 (d); 109.6 (d); 94.7 (s); 55.3 (t); 52.4 (d); 51.8 (q); 31.7 (t); 28.9 (t); 27.9 (q); 24.1 (t).

Synthesis of 1eQ and 1eR by Using DCI. To a stirred solution of the acid, **1eI** or **3** (1.25 mmol), in dry dioxane (10 mL), cooled to 0 °C, DCI (0.3 g, 1.87 mmol) was added. After 5 h, L-histidine methyl ester dihydrochloride (0.3 g, 1.25 mmol) and triethylamine (0.26 mL, 1.87 mmol) were added and the mixture was incubated at 80 °C for 8 h. Evaporation of the solvent under reduced pressure gave a solid that was purified by column chromatography using dichloromethane/methanol 9:1 as eluant to afford compounds **1eQ** or **1eR** (yields 80 and 70%, respectively).

***N*-[2-(1*H*-Imidazol-4-yl)ethyl]-4-(10-methyl-3-phenyl-5-oxo-5,10-dihydro-4*H*-indolo[3,2-*e*][1,2,3]triazolo[1,5-*a*]pyrimidin-4-yl)butanamide (1eJ).** To a stirred solution of the acid **1eI** (0.5 g, 1.25 mmol) in dry dioxane (10 mL), cooled to 0 °C, DCI (0.3 g, 1.87 mmol) was added. After 5 h, histamine-free base (0.2 g, 1.87 mmol) and triethylamine (0.26 mL, 1.87 mmol) were added and the mixture was incubated at 50 °C for 1 h. Evaporation of the solvent under reduced pressure gave a solid that was purified by column chromatography using dichloromethane/methanol 9:1 as eluant to afford compound **1eJ** (0.35 g, 0.7 mmol). Yield 56%, mp 207 °C. IR: 3360 (NH), 1716 (*C*═O), 1681 (*C*═O) cm^{-1}. ^1H NMR ppm: 8.50 (d, $J = 7.3$ Hz, 2H, H-2′ and H-6′); 8.09 (d, $J = 7.3$ Hz, 1H, H-6); 7.65 (t, $J = 7.3$ Hz, 1H, NHCH$_2$); 7.52–7.29 (m, 7H, H-7, H-8, H-9, H-3′, H-4′, H-5′ and H-2″); 6.75 (s, 1H, H-5″); 5.02 (t, $J = 6.6$ Hz, 2H, NCH$_2$); 3.93 (s, NCH$_3$); 3.36–3.17 (m, 4H, NHCH$_2$CH$_2$ and NHCH$_2$CH$_2$); 2.20 (t, $J = 7.4$ Hz, 2H, CH$_2$CO); 2.07–1.98 (m, 2H, CH$_2$CH$_2$CH$_2$). ^{13}C NMR ppm: 170.9 (s); 154.6 (s); 151.5 (s); 145.9 (s); 138.2 (s); 136.2 (s); 134.5 (d); 133.1 (s); 129.4 (d); 128.9 (d); 128.7 (s); 126.1 (d); 124.6 (d); 121.4

(d); 121.2 (s); 120.3 (d); 116.6 (d); 109.7 (d); 94.6 (s); 55.3 (t); 31.9 (t); 28.3 (t); 27.9 (q); 26.9 (t); 24.1 (t).

Biology. Methodology of the In Vitro Cancer Screen. The human tumor cell lines of the cancer screening panel are grown in RPMI 1640 medium containing 5% fetal bovine serum and 2 mM L-glutamine. For a typical screening experiment, cells are inoculated into 96-well microtiter plates in 100 μL at plating densities ranging from 5000 to 40000 cells/well, depending on the doubling time of individual cell lines. After cell inoculation, the microtiter plates are incubated at 37 °C, 5% CO_2, 95% air, and 100% relative humidity for 24 h prior to addition of experimental drugs. After 24 h, two plates of each cell line are fixed in situ with TCA, to represent a measurement of the cell population for each cell line at the time of drug addition (Tz). Experimental drugs are solubilized in DMSO at 400-fold the desired final maximum test concentration and stored frozen prior to use. At the time of drug addition, an aliquot of frozen concentrate is thawed and diluted to twice the desired final maximum test concentration with complete medium containing 50 μg/mL gentamicin. Additional four, 10-fold, or ½ log serial dilutions are made to provide a total of five drug concentrations plus control. Aliquots of 100 μL of these different drug dilutions are added to the appropriate microtiter wells already containing 100 μL of medium, resulting in the required final drug concentrations.

Following drug addition, the plates are incubated for an additional 48 h at 37 °C, 5% CO_2, 95% air, and 100% relative humidity. For adherent cells, the assay is terminated by the addition of cold TCA. Cells are fixed in situ by the gentle addition of 50 μL of cold 50% (w/v) TCA (final concentration, 10% TCA) and incubated for 60 min at 4 °C. The supernatant is discarded, and the plates are washed five times with tap water and air-dried. Sulforhodamine B (SRB) solution (100 μL) at 0.4% (w/v) in 1% acetic acid is added to each well, and plates are incubated for 10 min at room temperature. After staining, unbound dye is removed by washing five times with 1% acetic acid and the plates are air-dried. Bound stain is subsequently solubilized with 10 mM trizma base, and the absorbance is read on an automated plate reader at a wavelength of 515 nm. For suspension cells, the methodology is the same except that the assay is terminated by fixing settled cells at the bottom of the wells by gently adding 50 μL of 80% TCA (final concentration, 16% TCA). Using the seven absorbance measurements [time zero, (Tz), control growth, (C), and test growth in the presence of drug at the five concentration levels (Ti)], the percentage growth is calculated at each of the drug concentrations levels. Percentage growth inhibition is calculated as

$$[(\mathrm{Ti}-\mathrm{Tz})/(\mathrm{C}-\mathrm{Tz})]\times 100 \text{ for concentrations for which } \mathrm{Ti}\geq \mathrm{Tz}$$

$$[(\mathrm{Ti}-\mathrm{Tz})/\mathrm{Tz}]\times 100 \text{ for concentrations for which } \mathrm{Ti}<\mathrm{Tz}$$

Three dose−response parameters are calculated for each experimental agent. Growth inhibition of 50% (GI_{50}) is calculated from $[(\mathrm{Ti}-\mathrm{Tz})/(\mathrm{C}-\mathrm{Tz})]\times 100 = 50$, which is the drug concentration, resulting in a 50% reduction in the net protein increase (as measured by SRB staining) in control cells during the drug incubation. The drug concentration resulting in total growth inhibition (TGI) is calculated from Ti = Tz. The LC_{50} (concentration of drug resulting in a 50% reduction in the measured protein at the end of the drug treatment as compared to that at the beginning) indicating a net loss of cells following treatment is calculated from $[(\mathrm{Ti}-\mathrm{Tz})/\mathrm{Tz}]\times 100 = -50$. Values are calculated for each of these three parameters if the level of activity is reached; however, if the effect is not reached or is exceeded, the value for that parameter is expressed as greater or less than the maximum or minimum concentration tested.

Adriamycin was tested with each screening run as a quality control measure. This is done to establish the ability of the screen to generate information relevant to mechanism of growth inhibition/cell killing. It is not a reference compound that has unique importance for the compounds.

Acknowledgment. This work was financially supported by Ministero dell'Università e della Ricerca. We thank the National Cancer Institute, especially Dr. V. L. Narayanan, Dr. R. Shoemaker, and their teams, for the antitumor tests reported in this paper and for the helpful discussions.

Supporting Information Available: Elemental analyses for all compounds and table with full biological data. This material is available free of charge via the Internet at http://pubs.acs.org.

References

(1) (a) Aivasashvilli, V. A.; Beabealashvilli, R. S. Sequence-specific inhibition of RNA elongation by actinomycin D. *FEBS Lett.* **1983**, *160*, 124–128. (b) Lane, M. J.; Dabrowiak, J. C.; Vournakis, J. Sequence specificity of actinomycin D and Netropsin binding to pBR322 DNA analyzed by protection from DNase I. *Proc. Natl. Acad. Sci. U.S.A.* **1983**, *80*, 3260–3264. (c) Fox, K. R.; Waring, M. DNA structural variations produced by actinomycin and distamycin as revealed by DNAase I footprinting. *Nucleic Acids Res.* **1984**, *12*, 9271–9285. (d) Phillips, D. R.; Crothers, D. M. Biochemistry Kinetics and sequence specificity of drug-DNA interactions: an in vitro transcription assay. *Biochemistry* **1986**, *25*, 7355–7362. (e) Goodisman, J.; Rehfuss, R.; Ward, B.; Dabrowiak, J. C. Site-specific binding constants for actinomycin D on DNA determined from footprinting data. *Biochemistry* **1992**, *31*, 1046–1058.

(2) (a) Patel, D. J. Peptide antibiotic-oligonucleotide interactions. Nuclear magnetic resonance investigations of complex formation between actinomycin D and d-ApTpGpCpApT in aqueous solution. *Biochemistry* **1974**, *13*, 2396–2402. (b) Liu, X.; Chen, H.; Patel, D. J. Solution structure of actinomycin−DNA complexes: Drug intercalation at isolated G-C sites. *J. Biomol. NMR* **1991**, *1*, 323–347. (c) Brown, D. R.; Kurz, M.; Kearns, D. R.; Hsu, V. L. Formation of multiple complexes between actinomycin D and a DNA hairpin: Structural characterization by multinuclear NMR. *Biochemistry* **1994**, *33*, 651–664.

(3) (a) Sobell, H. M.; Jain, S. C.; Sakore, T. D.; Nordman, C. E. Stereochemistry of actinomycin−DNA binding. *Nature* **1971**, *231*, 200–205. (b) Sobell, H. M.; Jain, S. C. Stereochemistry of actinomycin binding to DNA. II. Detailed molecular model of actinomycin−DNA complex and its implications. *J. Mol. Biol.* **1972**, *68*, 21–34. (c) Kamitori, S.; Takusagawa, F. Crystal structure of the 2:1 complex between d(GAAGCTTC) and the anticancer drug actinomycin D. *J. Mol. Biol.* **1992**, *225*, 446–456. (d) Kamitori, S.; Takusagawa, F. Multiple binding modes of anticancer drug actinomycin D: X-ray, molecular modeling, and spectroscopic studies of $d(GAAGCTTC)_2$−actinomycin D complexes and its host DNA. *J. Am. Chem. Soc.* **1994**, *116*, 4154–4165.

(4) (a) Rill, R. L.; Marsch, G. A.; Graves, D. E. 7-Azido-actinomycin D: Photoaffinity probe of the sequence specificity of DNA binding by actinomycin D. *J. Biomol. Struct. Dyn.* **1989**, *7*, 591–605.

(5) Lian, C. Y.; Robinson, H.; Wang, A. H. J. Structure of actinomycin D bound with $(GAAGCTTC)_2$ and $(GATGCTTC)_2$ and its binding to the $(CAG)_n$:$(CTG)_n$ triplet sequence by NMR analysis. *J. Am. Chem. Soc.* **1996**, *118*, 8791–8801.

(6) Bailey, S. A.; Graves, D. E.; Rill, R.; Marsch, G. Influence of DNA base sequence on the binding energetics of actinomycin D. *Biochemistry* **1993**, *32*, 5881–5887.

(7) Lauria, A.; Diana, P.; Barraja, P.; Almerico, A. M.; Cirrincione, G.; Dattolo, G. Pyrrolo[3,4-*e*][1,2,3]triazolo[1,5-*a*]pyrimidine and pyrrolo[3,4-*d*][1,2,3]-triazolo[1,5-*a*]pyrimidine. New tricyclic ring systems of biological interest. *J. Heterocycl. Chem.* **2000**, *37*, 747–750.

(8) Lauria, A.; Diana, P.; Barraja, P.; Montalbano, A.; Cirrincione, G.; Dattolo, G.; Almerico, A. M. New tricyclic systems of biological interest. Annelated 1,2,3-triazolo[1,5-*a*]pyrimidines through domino reaction of 3-azidopyrroles and methylene active nitriles. *Tetrahedron* **2002**, *58*, 9723–9727.

(9) Lauria, A.; Patella, C.; Diana, P.; Barraja, P.; Montalbano, A.; Cirrincione, G.; Dattolo, G.; Almerico, A. M. A new tetracyclic ring system of biological interest. Indolo[3,2-*e*][1,2,3]triazolo[1,5-*a*]pyrimidines through domino reaction of 2-azidoindole. *Heterocycles* **2003**, *60*, 2669–2675.

(10) Lauria, A.; Patella, C.; Diana, P.; Barraja, P.; Montalbano, A.; Cirrincione, G.; Dattolo, G.; Almerico, A. M. A synthetic approach to new polycyclic ring system of biological interest through domino reaction: indolo[2,3-*e*][1,2,3]triazolo[1,5-*a*]pyrimidine. *Tetrahedron Lett.* **2006**, *47*, 2187–2190.

(11) Web address: http://www.ccdc.cam.ac.uk.

(12) Web address: http://www.rcsb.org/pdb.

(13) Web address: http://www.scripps.edu/pub/olson-web/doc/autodock.

(14) Morris, G. M.; Goodsell, D. S.; Halliday, R. S.; Huey, R.; Hart, W. E.; Belew, R. K.; Olson, A. J. Automated docking using Lamarckian genetic algorithm and an empirical binding free energy function. *J. Comput. Chem.* **1998**, *19*, 1639–1662.

(15) Lauria, A.; Patella, C.; Diana, P.; Barraja, P.; Montalbano, A.; Cirrincione, G.; Dattolo, G.; Almerico, A. M. MADoSPRO: A new approach to molecular modeling studies on a series of DNA minor groove binders. *QSAR Comb. Sci.* **2006**, *25*, 252–262.

(16) (a) See, for example, Doleschall, G.; Lempert, K. Mechanism of carboxyl condensations by carbodiimides. *Tetrahedron Lett.* **1963**, 1195–1199. (b) Hegarty, A. F.; McCormack, M. T.; Ferguson, G.; Roberts, P. J. Isolation and reactivity of a model for the carbodiimide-carboxylic acid adduct. *O*-Benzoyl-*N*,*N*-dimethyl-*N*′-(*N*-methyl-2,4-dinitroanilino)isourea. *J. Am. Chem. Soc.* **1977**, *99*, 2015–2016.

(17) Mikolajczyk, M.; Kielbasinski, P. Recent developments in the carbodimide chemistry. *Tetrahedron* **1981**, *37*, 233–284.

(18) (a) Grever, M. R.; Sherpartz, S. A.; Chabner, B. A. The National Cancer Institute: Cancer drug discovery and development program. *Semin. Oncol.* **1992**, *19*, 622–638. (b) Monks, A. P.; Scudiero, D. A.; Skehan, P.; Shoemaker, R.; Paull, K. D.; Vistica, D.; Hose, C.; Langley, J.; Croniste, P.; Vaigro-Woiff, A.; Gray-Goodrich, M.; Campbell, H.; Mayo, J.; Boyd, M. R. Feasibility of a high-flux anticancer drug screen utilizing a derived panel of human tumor cell lines in culture. *J. Natl. Cancer Inst.* **1991**, *83*, 757–766. (c) Weinstein, J. N.; Meyers, T. G.; O'Connor, P. M.; Friend, S. H.; Fornace, A. J., Jr.; Kohn, K. W.; Fojo, T.; Bates, S. E.; Rubinstein, L, V.; Anderson, N. L.; Boulamwini, J. K.; van Osdol, W. W.; Monks, A. P.; Scudiero, D. A.; Sausville, E. A.; Zaharevitz, D. W.; Bunow, B.; Viswanadhan, V. N.; Johnson, G. S.; Wittes, R. E.; Paull, K. D. An information-intensive approach to the molecular pharmacology of cancer. *Science* **1997**, *275*, 343–349.

(19) Data available on line at http://dtp.nci.nih.gov/dtpstandard/cancerscreeningdata/index.jsp (code: NSC3053).

(20) Paull, K. D.; Shoemaker, R. H.; Hodes, L.; Monks, A.; Scudiero, D. A.; Rubistein, L.; Plowman, J.; Boyd, M. R., J. Display and analysis of patterns of differential activity of drugs against human tumor cell lines: Development of mean graph and COMPARE algorithm. *Natl. Cancer Inst.* **1989**, *81*, 1088–1092.

(21) Available online at http://spheroid.ncifcrf.gov/default.html and developed according to the following: Rabow, A. A.; Shoemaker, R. H.; Sausville, E. A.; Covell, D. G. Mining the NCI's tumor screening database: Identification of compounds with similar cellular activities. *J. Med. Chem.* **2002**, *45*, 818–840.

(22) Web address: http://www.ddl.unimi.it.

(23) Morris, G. M.; Goodsell, D. S.; Huey, R.; Olson, A. J. Distributed automated docking of flexible ligands to proteins: Parallel applications of AutoDock 2.4. *J. Comp.-Aided Mol. Des.* **1996**, *10*, 293–304.

(24) Solis, F. J.; Wets, R. J. Minimization by random search techniques. *Math. Oper. Res.* **1981**, *6*, 19–30.

JM700964U